M. Peszynska, Methane in subsurface: mathematical modeling and computational challenges, IMA Volumes in Mathematics and its Applications 156, Computational Challenges in the Geosciences, edited by Clint Dawson and Margot Gerritsen, Springer, ISBN 978-1-4614-7433-3, 2013

# METHANE IN SUBSURFACE: MATHEMATICAL MODELING AND COMPUTATIONAL CHALLENGES *

MALGORZATA PESZYNSKA†

**Abstract.** We discuss mathematical and computational models of two applications important for global climate and energy recovery involving the evolution of methane gas in the subsurface. In particular, we develop advanced models of adsorption occuring in coalbed methane recovery processes, and discuss the underlying conservation laws with non-standard terms. Next we describe the phase transitions relevant for modeling methane hydrates in subsea sediments where the major challenge comes from implementation of solubility constraints. For both applications we formulate the discretization schemes and outline the main challenges in convergence analysis and solver techniques. We also motivate the need for continuum and discrete models at porescale.

**Key words.** multiphase and multicomponent flow and transport, porous media, adsorption models, phase transitions, finite differences, methane hydrates, semi-smooth functions, semi-smooth Newton methods, hysteresis, coalbed methane, mean-field equilibrium models

**AMS(MOS) subject classifications.** 76S05, 65M06, 65M22, 74N30, 76V05, 80A30, 65M75

## 1. Introduction.

Methane is both a greenhouse gas and an energy resource. In this paper we discuss the challenges in computational modeling of methane in two applications important for global climate and energy studies, namely Enhanced Coalbed Methane (ECBM) recovery, and modeling methane hydrate evolution in subsea sediments (MH).

Coalbed methane is a form of natural gas extracted from coal beds. In recent decades it has become an important source of energy in the United States and other countries, and coal and methane are important energy resources exported from the US. In the ECBM technology, carbon dioxide and/or nitrogen or other gases are injected into unmineable coal seams to promote displacement and extraction of methane. Recent pilot projects in various countries evaluated ECBM as a potential carbon sequestration technology [140, 51, 148, 82, 135, 49, 46]. The technology appears promising but is associated with various uncertainties and hazards, not the least of which include incomplete understanding of the underlying processes and difficulties with carrying out experiments.

*published in [IMA 156, Computational Challenges, edited by Clint Dawson and Margot Gerritsen], Springer, ISBN 978-1-4614-7433-3, 2013.] The final publication is available at link.springer.com

† Oregon State University, Department of Mathematics, Corvallis, OR, 97331, mpesz@math.oregonstate.edu. Research presented in this paper was partially supported by the grants NSF 1115827 “Hybrid modeling in porous media”, NSF 0511190 “Model Adaptivity for Porous Media”, and DOE 98089 “Modeling, analysis, and simulation of preferential flow”.

Methane hydrates (MH), an ice-like substance containing methane molecules trapped in a lattice of water molecules, are present in large amounts along continental slopes and in permafrost regions and, therefore, are a possible source of energy [129, 3, 86, 47], and at the same time a potential environmental hazard [38, 33, 127, 57, 29]. There are recent initiatives by DOE's National Energy Technology Laboratory (NETL), in collaboration with the U.S. Geological Survey (USGS), and an industry consortium led by Chevron, in gas hydrate drilling, research expeditions [6], and observatories [5, 7] which help to evaluate methane hydrate as an energy resource. Although the existence of gas hydrates in nature has been known for many decades, our understanding of their potential impact on slope stability, the biosphere, carbon cycling, and climate change is still evolving.

In this paper we overview the many open mathematical and computational questions that arise for these applications. They are relatively unknown to the mathematical and numerical community. We first overview their traditional continuum models which are systems of partial differential equations (PDEs) at mesoscale, i.e., lab or field scale. See Section 2 for notation, and Sections 3 and 4 for ECBM and MH models, respectively. Since these PDEs are nonlinear and coupled, no general theory of well-posedness or of convergence of approximation schemes is available. However, some analyses can be pursued for submodels of ECBM and MH, and their structure calls for a family of related mathematical and computational techniques and solvers. For the latter, some techniques originally developed for optimization are emerging as effective methods for solving nonlinear problems with inequality constraints and piecewise smooth nonlinearities.

The accuracy of computational models depends on the ability of the physical models themselves to describe all relevant phenomena and on the precision of their data. One common theme for ECBM and MH models is that they describe metastable phenomena such as adsorption and phase transitions whose physics may be either poorly understood or difficult to capture at mesocale. In addition, these evolution phenomena affect the porescale which in turn changes the flow and transport characteristics. In Section 5 we propose some models at porescale which can help to overcome the limitations of continuum modeling and provide a look-up library for the missing experimental data. In the future these models can be combined with the continuum models in static or dynamic hybrid schemes.

**2. Processes and continuum models.** The models of methane evolution must account for multiple phases and multiple components evolving in time in a porous reservoir $\Omega \subset \mathbb{R}^d$, $1 \leq d \leq 3$ under the earth surface of depth $D(\mathbf{x}), \mathbf{x} \in \Omega$, and porosity $\phi$ and permeability $K$. Recall that $\phi$ is a positive scalar, and $K$ is a uniformly positive definite tensor. Also, let $P, T$ denote pressure and temperature. Multiphase multicomponent flow and

transport models are generally coupled systems of nonlinear PDEs with additional volume, capillary, and thermodynamic constraints; see standard developments in [67, 45, 28].

The mass conservation equations written per each component $C$ read

$$\overbrace{\mathbf{Sto}_C}^{storage} + \overbrace{\mathbf{Adv}_C}^{advection} + \overbrace{\mathbf{Diff}_C}^{diffusion} = \overbrace{q_C}^{source}, \text{ in } \Omega, \tag{2.1}$$

in which the individual terms depend on the component $C$ under study, on the process, and its scale. Alternatively, one can write such equations per each component $C$ and each phase $p$, and account for the transfer of mass of a component between phases. Data for this dynamics is hard to obtain experimentally; however, it can be provided by porescale studies, see Section 5.

The definition of $\mathbf{Sto}_C$ is crucial for each application since it specifies how a component moves out of one form or phase, and whether the phase transitions or adsorption take place in equilibrium or via a kinetic model. The $\mathbf{Sto}_C$ terms include the time rate of change of all forms of the component $C$ dissolved in various flowing liquid or gas phases, present in a stationary phase such as adsorbed on a surface of porous skeleton or part of a gas hydrate crystal. In other words,

$$\mathbf{Sto}_C := \frac{\partial}{\partial t}(\phi N_C) := \frac{\partial}{\partial t}(\phi \sum_p \rho_p S_p \chi_{pC}).$$

Here we used the total mass concentration of a component $N_C$, with $S_p$ denoting the saturations/volume fractions, and $\rho_p$ density of phase $p$, respectively. We have $S_p \geq 0$, and $\sum_p S_p = 1$, and densities are given from an appropriate equation of state. Also, we used mass fractions of a component $C$ in phase $p$ denoted by $\chi_{pC}$. We have $\chi_{pC} \geq 0$ and for each phase $\sum_C \chi_{pC} = 1$.

Next we discuss the terms $\mathbf{Adv}, \mathbf{Diff}$. Their definitions depend on the application and scale. Typically, the diffusion/dispersion terms **Diff** are the divergence of diffusive fluxes formulated using Fick's law

$$\mathbf{Diff}_C := \nabla \cdot \left( \phi \sum_p \rho_p S_p D_{pC} \nabla \chi_{pC} \right), \tag{2.2}$$

and **Adv** includes divergence of mass fluxes

$$U_p = -K \frac{k_{rp}}{\mu_p} (\nabla P_p - \rho_p G \nabla D(\mathbf{x})), p = l, g, \tag{2.3}$$

$$\mathbf{Adv}_C := \nabla \cdot \sum_p \chi_{pC} \rho_p U_p, \tag{2.4}$$

with the velocities given via the multiphase extension of Darcy's law, where $k_{rp}, \mu_p$ denote relative permeability and viscosity of phase $p$ and $G$ the

gravity constant. In addition, the phase pressures of mobile phases $P_l, P_g$ are coupled via the capillary pressure relationship $P_g - P_l = P_c(S_l)$ given by Brooks-Corey relationships or van-Genuchten correlations [67, 56, 28].

The model (2.1) is very general; difficulties in its analysis and approximation arise from the presence of multiple components as well as from the various nonlinear couplings. Additionally, the data for some of these couplings are difficult to obtain, see Section 5. Special modeling constructs can be used to decrease the computational complexity associated, e.g., with multiple scales, non-equilibrium conditions, and metastability. On the other hand, these require additional care in numerical approximation.

We illustrate some of the relevant issues in a discussion of scalar (one-component) equations in $d = 1$ to follow. Throughout we rescale the variables and eliminate constants, e.g., $\phi$, to emphasize the qualitative rather than quantitative structure of the models.

First we consider similarities and differences in the generic scalar PDEs for ECBM and MH. In Sections 3 and 4 we elaborate on their details.

In the single-phase rescaled scalar version of (2.1) for ECBM we have

$$\frac{\partial}{\partial t}(\chi + \Upsilon) + \mathbf{Adv} + \mathbf{Diff} = 0, \tag{2.5}$$

where $\chi$ denotes the concentration or mass fraction of the mobile component, and $\Upsilon$ is that of the adsorbed amount. The connection between $\chi, \Upsilon$ and/or their rates has to be provided via an equilibrium, kinetic, or hysteretic relationship

$$(\chi, \Upsilon) \in F. \tag{2.6}$$

Here $F$ is a single- or multi-valued stationary or evolution relationship related to the graph of an adsorption/desorption isotherm.

For MH, the evolution of methane component is governed, in a simplified rescaled version, by

$$\frac{\partial}{\partial t}((1 - \Upsilon)\chi + R\Upsilon) + \mathbf{Adv} + \mathbf{Diff} = 0. \tag{2.7}$$

Here $(\chi, \Upsilon)$ are methane solubility and hydrate or gas saturation, respectively, and $R$ is a constant. The variables $(\chi, \Upsilon)$ are bound together by the volume and solubility constraints that can be written as (2.6).

The discretization of the models (2.5), (2.7) depends on the definition of $\mathbf{Adv}, \mathbf{Diff}$ and their relative significance. For example, for dominant diffusion, finite elements in space and implicit backward Euler schemes in time can be used. For dominant advection, conservative consistent finite difference schemes are needed, and the advection terms are typically handled explicitly in time. When both diffusion and advection are present we can use an operator splitting procedure.

For a simple $F$ in (2.6), fairly well-known results on the discretization and analyses are available. For complicated $F$, the handling of (2.6), especially for multi-valued relations and analysis are a challenge. In Sections 3 and 4 we provide details relevant to ECBM and MH; we focus on the representation and approximation of $F$ and discuss the associated stability and solver issues. In Section 5 we propose the use of hybrid computational models which can be used to obtain data for $F$ and other essential model ingredients.

Finally, the initial and boundary conditions need to be specified to close any system of PDEs and to discuss its well-posedness. However, analysis of either ECBM or MH has not been attempted, and coupled nonlinear systems of partial differential equations of mixed, variable, and degenerate type do not have a general well-posedness theory except for special submodels [125, 98, 10, 11, 25]. The lack of general theory makes the numerical approximation delicate; it is necessary to thoroughly understand each subproblem as well as the challenges of the coupled system, to the extent possible, before a particular numerical discretization method is selected and its results are used. Various simulators have been successfully implemented for typical multiphase multicomponent models, and these are based on carefully selected spatial discretization schemes and nonlinear solvers [77, 104, 97, 45, 138, 70, 2, 110, 4]. In the exposition below we discuss avenues for possible analyses and algorithmic extensions of some of these schemes.

**3. Transport with adsorption in ECBM.** Coalbeds have the form of coal *seams* surrounded by sandstone, gravel, mudstone or shales. The coal seams have a multiscale structure of microporous coal matrix interspersed with *cleats* i.e. fractures or macropores. The majority of transport occurs in the cleats accompanying the flow of gas and possibly of water, while the majority of storage occurs in the matrix where gases undergo diffusion and adsorption, close to supercritical conditions. For ECBM, the components are $C = M, D, N, (W)$ methane, carbon dioxide, nitrogen, and (for wet gas models) water. The phases in which these components can remain are $p = g, a, l$: gas, adsorbed gas, and liquid phase (for wet gas).

In a simple dry-gas model with $S_g = 1$ for ECBM with $C = M, D, N$, with $p = g, a$ we have

$$\chi_{gM} + \chi_{gD} + \chi_{gN} = 1, \tag{3.1}$$

$$\chi_{aM} + \chi_{aD} + \chi_{aN} = 1, \tag{3.2}$$

so that the equations (2.1) are written for the evolution of $N_M, N_D, N_N$.

When gases such as carbon dioxide are injected into coal seams, they make their way through the cleats into the micropore structure of the matrix. Here they preferentially adsorb, displacing methane from adsorption sites; subsequently, this methane is transported through cleats and is available for extraction. The predominant transport mechanism in cleats

(macropores) is that of advection while the transport into and out of the coal matrix occurs through diffusion into mesopores and micropores, where the gases undergo adsorption and desorption at the surface of the grains.

Adsorption is a surface phenomenon in which particles, molecules, or atoms of adsorbate attach to the surface of adsorbent. It has numerous technical applications ranging from water purification, chromatography, to drug delivery, and is fundamental in ECBM. There is current research on the nature and occurence of adsorption-desorption hysteresis [27, 122, 112], and competitive, or preferential adsorption [23, 24, 21, 123, 62, 55, 78]. Functional relationships that fit some of experimental data were proposed in [26, 27, 20, 91, 81, 126, 31], but comprehensive models are lacking.

**3.1. Adsorption models.** Consider now a relationship between $\chi := \chi_{gM}$ and $\Upsilon := \chi_{aM}$ that needs to be provided to complement (3.1), (3.2) for the methane component $C = M$. (Similar relationships are needed for $C = D, N$). Basic experimental models are usually given as equilibrium isotherms [1, 39] such as

$$\Upsilon = f(\chi), \tag{3.3}$$

where $f$ is a known smooth monotone increasing function which describes the surface coverage $\Upsilon$ of adsorbent depending on the gas or vapour pressure $\chi$ of adsorbate, at constant temperature, in equilibrium. For example, the well-known Langmuir type-I isotherm [1] has the form

$$\Upsilon = f(\chi) = \Upsilon^{max} \frac{b\chi}{1 + b\chi}, \tag{3.4}$$

where $b, \Upsilon^{max}$ are constants, and is derived from monolayer assumption and equality of adsorption and desorption rates. This isotherm applies well in a variety of microporous, meso-to macro-porous media in sub, near-, and supercritical conditions [39, 62]. Note that $\Upsilon = f(\chi)$ is smooth concave, increasing, and Lipschitz.

An alternative to the equilibrium model (3.3) is the kinetic model

$$\frac{d\Upsilon}{dt} = r(f(\chi) - \Upsilon), \tag{3.5}$$

in which $\Upsilon$ is an exponential follower (with rate $r$) of the equilibrium model $f(\chi)$. See [14, 16, 15, 35, 36] where numerical schemes for (2.5) and (3.3) or (3.5) were proposed and analyzed. Difficulties arise if the isotherm is not Lipschitz in (3.3)–(3.5) but this case is not relevant for ECBM. See also [133] for a discussion of stability of the Godunov (upwind) method for the equilibrium case and the one for kinetic model, as well as their relationship in $d = 1$.

We discuss now the model for $\mathbf{Diff} \sim 0$, $\mathbf{Adv} = \nabla \cdot \chi$. Then (2.5) is of hyperbolic type and can be rewritten as a scalar conservation law via a

change of variable $w = \chi + \Upsilon$

$$w_t + \nabla \cdot g(w) = 0, \tag{3.6}$$

with an increasing and convex flux function $g \sim (I + f)^{-1}$. It is well known [71] that its solutions develop singularities in finite time from smooth initial data. An appropriate numerical method needs to be conservative and stable. For example, this is satisfied by the Godunov method, written here in primary variables for (2.5)

$$\chi_j^n + \Upsilon_j^n + \lambda(\chi_j^{n-1} - \chi_{j-1}^{n-1}) = \chi_j^{n-1} + \Upsilon_j^{n-1}, \tag{3.7}$$

where $\lambda = \frac{k}{h}$, $k$ is the time step, and $h$ is the spatial discretization parameter. The discretization is defined at the discrete spatial and temporal points $x_j = jh, t_n = nk$. The scheme is stable provided $\lambda \leq 1 + f'(\chi_j^n)$, which is easy to satisfy if, e.g., $\lambda \leq 1$.

Strictly speaking, a Godunov scheme for (3.6) is entirely explicit and does not require a solution of any global linear or nonlinear system. However, the scheme in (3.7) is not, since it requires solving

$$\chi_j^n + \Upsilon_j^n = \chi_j^n + f(\chi_j^n) = A_j, \tag{3.8}$$

where $A_j := -\lambda(\chi_j^{n-1} - \chi_{j-1}^{n-1}) + \chi_j^{n-1} + \Upsilon_j^{n-1}$ is known from the previous time step, and where we substituted (3.3) in (2.5).

Solving of (3.8) has to be done only locally at every grid point. In fact, for some isotherms, e.g., Langmuir, the algebraic form of (3.8) is very simple and (3.8) can be solved explicitly for $\chi_j^n$. In other cases, a simple local Newton iteration suffices, since $I + f$ is a smooth bijective function. To avoid unphysical negative iterates for $\chi_j^n$ it is sufficient to use an initial guess determined from the zero of the linear model of $f$ at 0, i.e., of $f(\chi) \approx \Upsilon^{max} b \chi$.

Now consider the non-equilibrium case, i.e., when (2.5) is complemented by (3.5). Formally we have to solve now, in addition to (3.7), a coupled ODE defined at every grid point

$$\Upsilon_j^n = \Upsilon_j^{n-1} + kr\left(f(\chi_j^{\tilde{n}}) - \Upsilon_j^{\bar{n}}\right), \tag{3.9}$$

where $\bar{n}, \tilde{n}$ denote either $n$ or $n-1$. For small $r$ and moderate $f'$ one can find a sufficiently small $k$ to ensure the conditional stability of the explicit solution. For large $r$ the system is stiff and therefore calls for implicit treatment with $\bar{n} = \tilde{n} = n$ so that

$$\chi_j^n + \Upsilon_j^n = A_j, \tag{3.10}$$

$$-krf(\eta_j^n) + (1 + kr)\Upsilon_j^n = B_j = \Upsilon_j^{n-1}. \tag{3.11}$$

where $A_j, B_j$ are known from previous time step. Its solvability for a monotone $f$ is analyzed similarly to (3.8).

In what follows we first discuss the extensions to the basic scalar models defined above and next we discuss the multicomponent case.

**3.2. Diffusion into micropores and transport with memory terms.** In ECBM, the predominantly advective transport in cleats is accompanied by a range of diffusive phenomena in which the molecules of methane and carbon dioxide migrate and get adsorbed to the meso- and micro-pores of the coal. This is known to affect the molecular structure of coal matrix and leads to the experimentally observed phenomena such as coal matrix swelling which has a distinct kinetic character [90, 24, 123, 150, 78, 137].

The micropore and mesopore diffusion have been included in the classical bidisperse model [114, 65] extended to include adsorption in micropores in [26] and to realistic gas transport models [124], with ECBM-related experimental work on the rates of kinetics in [20]. See also [65, 114, 123, 26].

These models include in the $\mathbf{Sto}_C$ the quantity $\Upsilon$ living in micropores which is governed by its own diffusion equation at a lower scale. Thus, $\Upsilon$ is related to $\chi$ via a convolution

$$\frac{\partial \Upsilon}{\partial t} := \frac{\partial \chi}{\partial t} * \beta := \int_0^t \frac{\partial \chi}{\partial t}(t-s)\beta(s)ds. \tag{3.12}$$

Here $\beta \in C^1(0,T)$ is a weakly singular or bounded monotone decreasing kernel, i.e., is locally integrable, with $\beta' \leq 0$. When (3.12) models the micropore diffusion, $\beta(t) \sim t^{-1/2}$ close to $t = 0$. Some approximations [26, 20] use $\beta(t) = \beta_{exp}(t) := rexp(-rt)$ with a rate $r > 0$. Note also that the kinetic model (3.5) can be written as a mild generalization of (3.12) where, up to terms associated with the initial values of $\Upsilon$, $\Upsilon := \frac{\partial f(\chi)}{\partial t} * \beta$ with $\beta = \beta_{exp}$.

Combine now (2.5),(3.12) written together as

$$\frac{\partial \chi}{\partial t} + \frac{\partial \chi}{\partial t} * \beta + \mathbf{Adv} + \mathbf{Diff} = 0. \tag{3.13}$$

We recognize (3.13) as a double-porosity model [12, 59] for slightly compressible flow in oil- and gas reservoirs with fractures and fissures. Also, see [99] for other multiscale analyses leading to a system whose part is similar to (3.13), and [95, 105, 106, 41, 100, 147] for other computational models of double-porosity.

To properly approximate the solutions to (3.13) we need to discretize the term $\frac{\partial \chi}{\partial t} * \beta$; here the difficulty is the singularity of $\beta$ at $t = 0$. An appropriate discretization based on product integration rules was proposed, and the analysis of the resulting scheme for $\mathbf{Adv} \equiv 0$ carried out, in [107, 105].

However, in ECBM, we have $\mathbf{Diff} \equiv 0, \mathbf{Adv} \not\equiv 0$. Now the appropriate numerical approximation of (3.13) falls in the class of schemes for scalar conservation laws with memory. In our recent work in [94] we developed convergence analysis for a scheme combining the Godunov scheme with the approximation of memory terms similar to that in [105, 107]. These

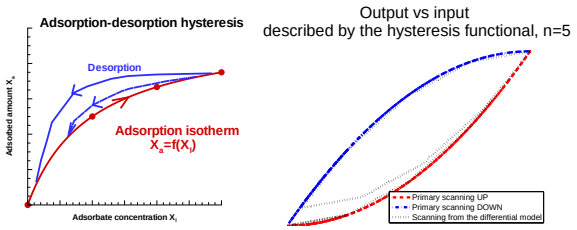


FIG. 1. *Left: adsorption/desorption hysteresis similar to those in [55, 112, 122]. Right: a graph obtained with a Preisach model of hysteresis with* $|A| = 5$ *as described in [98]*

results relate to the analysis of problems with memory in [30, 52] in which the smoothing effects of the memory terms upon the solution to (3.13) are discussed. These in turn can be interepreted in ECBM from the physical standpoint as follows: the presence of the subscale diffusion into and out of the coal matrix has the potential to smooth out any sharp fronts, should they arise in the cleat.

As concerns multicomponent transport with memory, practical implementation results for (3.13) were reported for ECBM in [123, 149]. More accurate models combining multi-porosity with IAS adsorption can be developed, see Section 3.4.

**3.3. Adsorption Hysteresis.** Desorption is a mechanism reverse to adsorption. In equilibrium both are described by the same isotherm (3.3). The adsorption hysteresis occurs in special non-equilibrium circumstances when these processes are described by different isotherms, see Figure 1. The many theories that explain adsorption hysteresis do so either by studying phenomena in a single pore in the so-called independent pore theories, or by attributing the hysteresis to the presence of a complex interconnected pore network [13]. The first class of theories studies metastable states such as superheating and undercooling of a fluid undergoing phase transition in a single pore as well as the lack of symmetry of the gas-liquid interface upon filling and emptying. The second mechanism studies adsorption in pore networks and the pore blocking and obstruction of desorption by the liquid remaining in the narrow necks of the pores [44, 115].

As concerns continuum computational models of adsorption hysteresis, one can proceed in (at least) one of two ways. The first as in [122] uses separate isotherms $f_j, j = 1, 2$ as in (3.4), each with its own parameters $\Upsilon_j^{max}, b_j$. However, it is not clear from [122] how the intermediate scanning curves are created when the desorption occurs at an intermediate value of $\chi$ between the primary bounding curves; also, no analysis is available.

The second possibility is to consider a family of differential models of hysteresis [98, 96, 136] which is amenable to analysis. In the Preisach model of hysteresis, one generalizes (3.5) and considers a multivalued maximal

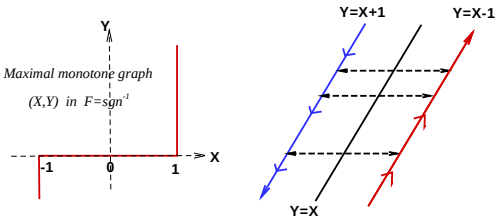


FIG. 2. *Construction of an elementary hysteresis loop which serves as a building block for more complicated graphs. Left: a graph $F$. Right: hysteresis loop using $F$.*

monotone graph $F$ instead of the function $f$ in the form

$$\frac{\partial \Upsilon}{\partial t} + F(\Upsilon - \chi) \ni 0. \tag{3.14}$$

This construction allows an unambiguous representation of primary bounding and secondary scanning curves and, thanks to the convex-concave properties of the resulting hysteresis graph (see Figure 1, right) it leads to well-posedness and higher regularity of solutions than those of usual conservation laws; see [98].

For terminology on monotone operators we refer to [125] and explain only briefly how (3.14) works to deliver, e.g., a graph such as in Figure 1, right. Consider $F = sgn^{-1}$, with domain $D_F := [-1, 1]$, see Figure 2. We can identify $F$ with its graph and write $F := \{-1\} \times (-\infty, 0) \cup (-1, 1) \times \{0\} \cup \{1\} \times (0, \infty)$. The relation (3.14) means that $\Upsilon - \chi$ remains in the domain of $F$, and that the rate $\Upsilon_t$ is either positive, negative, or zero, depending on whether $\Upsilon - \chi$ is equal to $-1$, $+1$, or is in $(-1, 1)$, respectively. Paraphrazing, given an increasing input $\chi$, the output $\Upsilon$ is allowed to either not change or increase along $\Upsilon = \chi - 1$. In contrast, for $\chi$ decreasing, $\Upsilon$ can only remain constant or to decrease along $\Upsilon = \chi + 1$.

Now, using $sgn^{-1}$ as a building block (but any other maximal monotone graph can be used), define $f_\alpha(s) := sgn^{-1}(\frac{2}{\alpha}s + 1)$, for some $\alpha > 0$, and let $\Upsilon_\alpha$ satisfy an analogue of (3.14) in which $F$ is replaced by $f_\alpha$. This allows one to construct a complicated convex-concave graph via $\Upsilon = \sum_{\alpha \in A} \Upsilon_\alpha$, in which $\mathcal{A} \subset \mathbb{R}_+$ is a finite collection of parameters; see the graph shown in Figure 1, right, with $|\mathcal{A}| = 5$. A more complicated, i.e. continuum set $\mathcal{A}$ can be used instead, but this is irrelevant for a computational model. See [98] for details.

Consider a numerical scheme for (2.5) coupled with (3.14); the difficulty here is in the understanding the differential inclusion in (3.14). This follows from the theory of evolution equations with monotone operators. We define the resolvent $J_\epsilon := (I + \epsilon F)^{-1}$ for any $\epsilon > 0$, and the Yosida approximation $F_\epsilon := \frac{1}{\epsilon}(I - J_\epsilon)$ to $F$. Both $J_\epsilon$ and $F_\epsilon$ are monotone Lipschitz functions with Lipschitz constants bounded by 1 and $\frac{1}{\epsilon}$, respectively.

We propose two avenues towards discretization of (3.14) beginning with $|\mathcal{A}| = 1$. First, we can use a regularized model for (3.14) $\frac{\partial \Upsilon_\epsilon}{\partial t} + F_\epsilon(\Upsilon_\epsilon - \eta) = 0$ in which we have replaced a multi-valued $F$ by the single-valued Yosida approximation $F_\epsilon$, and an inclusion by an equation. Its numerical approximation should be implicit because for $\epsilon \to 0$, the ODE is very stiff. Either way, the error will depend on $\epsilon$.

Second, we can consider an implicit in time discretization of (3.14)

$$\frac{\Upsilon_j^n - \Upsilon_j^{n-1}}{k} + F(\Upsilon_j^n - \chi_j^n) \ni 0. \tag{3.15}$$

This inclusion can be understood unambigously using the resolvent $J_k = (I + kF)^{-1}$. Multiply (3.15) by $k$ and subtract $\chi^n$ from both sides to see, after regrouping, that

$$\Upsilon_j^n - \chi_j^n + kF(\Upsilon_j^n - \chi_j^n) \ni \Upsilon_j^{n-1} - \chi_j^n.$$

Now apply the resolvent $J_k$ to both sides to get

$$\Upsilon_j^n - \chi_j^n = J_k(\Upsilon_j^{n-1} - \chi_j^n). \tag{3.16}$$

This form, coupled with (3.7) is now amenable to analysis and implementation. The analysis reveals that the scheme is stable as long as $\lambda \leq 1$. However, questions remain as concerns the (order of) consistency of the scheme, see [93].

Now we describe how to solve (3.16). Substitute (3.16) in (3.7) to obtain a local nonlinear problem to be solved at each grid point $j$

$$H(\chi_j^n) := \chi_j^n + \chi_j^n + J_k(\Upsilon_j^{n-1} - \chi_j^n) = A_j. \tag{3.17}$$

Since $2I + J_k$ is bijective, (3.17) is uniquely solvable. Since $H$ is also piecewise linear and therefore, *semi-smooth*, the Newton's method will converge $q$-superlinearly; see [134], Prop. 2.12, 2.25.

Now consider the case when $|\mathcal{A}| > 1$. For each $\alpha \in \mathcal{A}$ we can choose a scheme based on Yosida approximation or on the resolvent. It appears most practical to use the latter scheme since it does not depend on the regularization parameter. Thus, per each grid point $j, n$, a local system of equations composed of (3.7), and $|\mathcal{A}|$ variants of (3.16), with a sparse Jacobian, have to be solved.

Finally, adapting the construction above to arbitrary shape scanning curves is part of our current work since the symmetry of the graph $F$ in may be undesirable from the point of view of applications; compare the graphs in Figure 1. Furthermore, multicomponent extensions are needed, see Section 3.4.

**3.4. Multicomponent transport with adsorption.** The models discussed in Sections 3.2 and 3.3 are scalar, i.e., are defined for only one mobile component $\chi$ interacting with one adsorbed component $\Upsilon$. In ECBM

we have, however, several interacting components such as $M$, $D$, and $N$. For multiple components several issues arise: one concerning numerical approximation and analysis, and another, concerning the data for (2.6).

We start with the first issue and discuss the multicomponent model as derived from (2.1). We assume for simplicity (3.1), (3.2) and ignore the presence of $C = N$ so that the nitrogen serves as a carrier only and does not get adsorbed. Further, let the flow displacement velocity $U_g \equiv const$ in the model be known. Thus we only consider equations for $C = D, M$. Further assume constant gas densities. Now, with rescaling, and $\mathbf{Adv}_C = \nabla \cdot (U_g \chi_{gC})$ and $\mathbf{Diff}_C = \nabla \cdot (D_{gC} \nabla \chi_{gC})$, we can write the equations for $C = M, D$, each of which is similar to (2.5)

$$\frac{\partial}{\partial t}(\chi_{gM} + \chi_{aM}) + \mathbf{Adv}_M + \mathbf{Diff}_M = 0, \tag{3.18}$$

$$\frac{\partial}{\partial t}(\chi_{gD} + \chi_{aD}) + \mathbf{Adv}_D + \mathbf{Diff}_D = 0. \tag{3.19}$$

To complete this model, we need relationships between $\chi_{aC}$ and $\Upsilon_{aC}$ for $C = M, D$. These extend either the equilibrium (3.3), kinetic (3.5), double-porosity, or hysteretic relationships from Sections 3.2, 3.3 and are coupled. For example, the equilibrium isotherm for $C = M$ depends on the other components $\Upsilon_M := \chi_{aM} = \chi_{aM}(\chi_{lM}, \chi_{lD})$ because the adsorption capacity of any porous system is finite and thus the species compete for available adsorption sites.

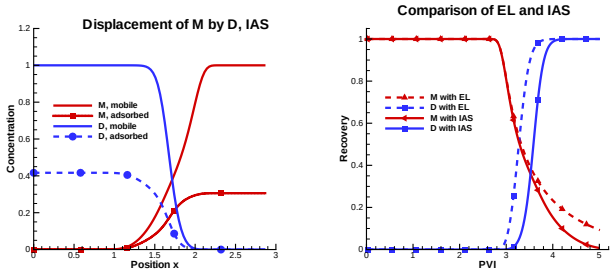


FIG. 3. *Left: illustration of competitive adsorption when methane $CH_4$ ($C = M$) initially present in the coal matrix is displaced by the injected carbon dioxide $CO_2$ ($C = D$) which adsorbs more strongly. Right: comparison of $CH_4/CO_2$ recovery using Extended Langmuir (EL) and Ideal Adsorbate Theory (IAS). Plotted are breakthrough curves with respect to pore volume injected (PVI). Both examples use physical parameters from [62, 123], with nitrogen $N_2$ ignored*

The functional form of the multicomponent isotherms could be obtained experimentally. However, the number of necessary experiments appears unpractical for systems with a large number of components. Instead, theoretical models for multicomponent mixtures have been proposed in the literature as extensions of single-component isotherms. For example, an

extension of the Langmuir model is

$$\Upsilon_M = f_{MD}(\chi_M, \chi_D) := \Upsilon_M^{max} \frac{b_M \chi_M}{1 + b_M \chi_M + b_D \chi_D}, \tag{3.20}$$

with a similar equilibrium isotherm $f_{DM}$ written for $\Upsilon_D$, where we have used the simplified notation $\chi_C := \chi_{gC}; \Upsilon_C := \chi_{aC}$.

Assuming that the isotherms $f_{MD}, f_{DM}$ are given, we consider briefly the numerical approximation of the equilibrium model. Here we can use an appropriate extension of the first order Godunov scheme (3.7) for systems. Since the transport term itself is linear, we can simply use the upwind method, and the lack of an exact Riemann solver for the system is not an issue. However, we need to resolve the coupling in the storage terms which, for **Diff** $\equiv 0$, extends (3.8) to a system of coupled algebraic equations

$$\chi_{M,j}^n + \Upsilon_{M,j}^n = \chi_{M,j}^n + f_{MD}(\chi_{M,j}^n, \chi_{D,j}^n) = A_{M,j}, \tag{3.21}$$

$$\chi_{D,j}^n + \Upsilon_{D,j}^N = \chi_{D,j}^n + f_{DM}(\chi_{M,j}^n, \chi_{D,j}^n) = A_{D,j}. \tag{3.22}$$

See an illustration of preferential adsorption and displacement of one component by the other in Figure 3.

However, the extended Langmuir model (EL) (3.20) appears thermodynamically inconsistent [39]. A consistent more accurate model follows from the Ideal Adsorbate Solution (IAS) theory [39, 149]. IAS takes advantage of the easy-to-obtain single component isotherms and derives a system of algebraic equations from the equality of potentials similar to vapor-liquid equilibria represented by Raoult's law. Theoretically, this system needs to be solved in a pre-processing step to provide lookup table values for $f_{MD}, f_{DM}$. In fact, however, this step can be easily combined with solving (3.21)–(3.22). An illustration of the nontrivial difference between the use of EL and IAS is given in Figure 3.

Having settled on an equilibrium model, we need to see if it is amenable to kinetic, double-porosity, and hysteresis extensions. Consider first an extension of a kinetic model (3.5) to the multicomponent case; it readily follows from a given equilibrium model but we now need to know various rates $r_M, r_D$ which are hard to measure and may be actually functions rather than constants. In addition, double-porosity models and/or hysteresis models are more difficult to conceptualize, and their analysis and numerical approximation is more complex. Overall, it appears that one avenue available for the study of these complex multicomponent processes is to consider a completely different characterization of adsorption. See Section 5 for a discussion of adsorption at porescale.

**4. Methane Hydrate models.** For methane hydrates [76, 48] one considers two mobile fluid phases $l, g$ (brine, gas) and an immobile hydrate phase $h$ (hydrate). In addition to the methane $M$, the main components of the fluids in the porespace are water $W$ and salt $S$. Usually the pore

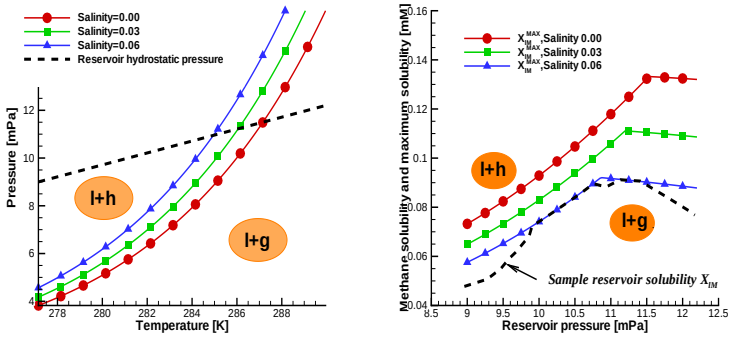


FIG. 4. *Left:* $P - T$ *diagram for hydrates used in [101, 66]. Right: Maximum solubility* $\chi_{lM}^{max}$ *diagram for reservoir conditions*

space is mainly saturated with water phase, with only a small amount of methane in the gas or hydrate phase being present.

The distribution of components between phases is governed by thermodynamics. Typically we have

$$\begin{aligned} \chi_{gM} &= 1, \quad \text{(gas phase contains methane only)}, \\ \chi_{hM} + \chi_{hW} &= 1, \quad \text{(both known for a fixed hydrate nuumber)}, \\ \chi_{lM} + \chi_{lW} + \chi_{lS} &= 1, \quad \text{(unknown variables)}. \end{aligned}$$

Phase behavior data for methane hydrates is available from various sources albeit the models vary slightly in complexity and detail. In [101] we used phase behavior data from [131, 48, 127] for i) the equilibrium (melting/dissociation) pressure $P^{EQ} = P^{EQ}(T, \chi_{lS})$ and ii) maximum solubility $\chi_{lM}^{max}(P, T, \chi_{lS})$ of methane $M$ in liquid phase $p = l$; see Figure 4 for illustration. Other thermodynamics properties needed in a comprehensive model follow from an equation of state (EOS) [127, 48, 131, 34, 43, 42].

**4.1. Simplified one equation model.** The simple model (2.7) explains well the main modeling constructs and solubility constraints. It can be obtained under the following simplifying assumptions. First, assume that $P, T$ are given in a reservoir and that they follow a static distribution due to hydrostatic and geothermal gradients, respectively. Next, ignore the dependence of $P^{EQ}$ and $\chi_{lM}^{max}$ on the salinity $\chi_{lS}$, and set $\chi_{lS} \equiv const$. If pressure and temperature are low enough i.e., above a certain depth below the earth surface, only a hydrate can form, see Figure 4, left. On the other hand, below a certain critical depth, the pressure and temperature are higher and only free gas can form. Finally, the hydrate and/or free gas can form only if the amount of methane $N_M$ exceeds the amount associated with the maximum solubility at that depth, see Figure 4, right.

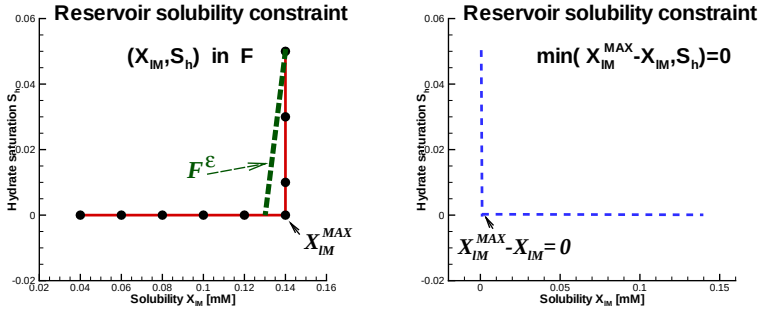


FIG. 5. *Left: representation of a phase constraint between* $\chi_{lM}^{max}$ *and* $S_h$ *using the graph* $F$*. Also, its regularization* $F^\epsilon$ *that was used in a kinetic model in [66]. Right: the mirror image of* $F$ *and representation of the same constraint using the* min *function as in* (4.5)

In the hydrate zone we have $S_g = 0$ and $1 \geq S_l > 0$ with $1 > 1 - S_l = S_h \geq 0$. Assume constant $\phi, \rho_l, \rho_h, \chi_{hM}$. The equation (2.1), after rescaling, becomes then

$$\frac{\partial}{\partial t}((1 - S_h)\chi_{lM} + S_h R_h) + \mathbf{Adv}_M + \mathbf{Diff}_M = 0 \tag{4.1}$$

where $R_h \equiv const$, and where we have used $S_h + S_l = 1$. We now need a relationship between $S_h$ and $\chi_{lM}$, or their rates.

In equilibrium between the liquid and hydrate phases, we have the solubility constraint $\chi_{lM} \leq \chi_{lM}^{max}$ and the volume constraint $S_h \geq 0$. At most one of these inequalities can be sharp which is expressed by $S_h(\chi_{lM}^{max} - \chi_{lM}) = 0$. This can be also written as $(\chi_{lM}, S_h) \in F := [0, \chi_{lM}^{max}) \times \{0\} \cup \{\chi_{lM}^{max}) \times (0, 1)$, see Figure 5.

A similar model can be formulated in the free gas zone for liquid-gas phase equilibria where $S_h = 0, S_l > 0, S_g \geq 0$. Such a model in which free gas phase may appear or disappear resembles the gas component part of the black-oil model [77, 97], carbon sequestration models such as [111], or hydrogen storage [50].

$$\frac{\partial}{\partial t}((1 - S_g)\chi_{lM} + S_g R_g) + \mathbf{Adv}_M + \mathbf{Diff}_M = 0 \tag{4.2}$$

where $R_g \equiv const$. We note that the constants $R_h, R_g$ exceed $\chi_{lm}^{max}$ by about two orders of magnitude, a fact that is useful in the analysis of the numerical scheme for (4.1), (4.2).

Before we propose the discretization, we comment on the transport terms in these simplified equations. In (4.1) the hydrate phase is immobile and methane can be transported only by diffusion within brine. In (4.2) the gas phase can be mobile for large enough $S_g$; in addition, transport

occurs by diffusion within the liquid phase. Overall, advection may be negligible if the system is close to hydrostatic equilibrium. On the other hand, diffusion may be negligible when the system changes rapidly away from equilibrium due to the heat or gas fluxes across the boundaries. See [145, 75, 144, 33, 34, 88, 34, 33, 79] for various examples and scenarios with different time and spatial scales of interest; see also [101].

**4.2. Numerical model for the simplified case.** Now we discuss the numerical approximation of the phase equilibria in the generic model (2.7) which includes (4.1) and (4.2) as special cases with $\Upsilon := S_h, R = R_h$, and $\Upsilon := S_g, R = R_g$, respectively, and with $\chi := \chi_{lM}$.

We discretize (2.7) in time and space and get

$$\begin{aligned}(1-\Upsilon_j^n)\chi_j^n + R\Upsilon_j^n + k\mathbf{Diff}_j^{\bar{n}} &= -k\mathbf{Adv}_j^{n-1} \\ &\quad + (1-\Upsilon_j^{n-1})\chi_j^{n-1} + R\Upsilon_j^{n-1}, \qquad (4.3)\\ (\chi_j^n, \Upsilon_j^n) &\in F. \qquad (4.4)\end{aligned}$$

The usual treatment is to handle the advection explicitly and diffusion implicitly so that $\bar{n} = n$, but in the exposition below we may use $\bar{n} = n-1$. The computational realization of (4.4) is the crux of the algorithm.

Following the ideas in [50] we express (4.4) by recognizing that the mirror image of $F$, see Figure 5, is a level curve of the "min" function so that (4.4) is equivalent to

$$\min(\chi^{max} - \chi_j^n, \Upsilon_j^n) = 0. \qquad (4.5)$$

This characterization of the graph $F$ now lends itself to a nonlinear iteration that can be applied to (4.3) and (4.5). Here we follow the ideas from [50] and consider a class of semi-smooth Newton methods described recently in [134]. For relevant background on complementarity conditions, see also [32, 60]. We outline this method below.

Let $\bar{n} = n-1$ so we can write out the system (4.3) and (4.5) that has to be resolved at each grid point $j, n$ as a local $2 \times 2$ system of equations

$$H(\chi_j^n, \Upsilon_j^n) = \mathbf{0} \equiv \left\{ \begin{array}{rcl} (1-\Upsilon_j^n)\chi_j^n + R\Upsilon_j^n & = & A_j \\ \min(\chi^{max} - \chi_j^n, \Upsilon_j^n) & = & 0, \end{array} \right. \qquad (4.6)$$

where $A_j$ is given from (4.3).

Now the problem (4.6) can be solved by Newton's iteration. However, we notice non-differentiability of the second component of $H$ across $\mathbb{R}^2 \supset A := \{(\chi, \Upsilon) : \Upsilon = \chi^{max} - \chi\}$. Away from that singularity, $H$ is smooth in both variables, and thus is a *semi-smooth function* on $B := \{(\chi, \Upsilon) : 0 \le \chi \le \chi^{max}, 0 \le \Upsilon < 1\}$, see [134], Prop. 2.25.

We can calculate the Jacobian $H'$ where it exists

$$H' := \begin{cases} M_1 := \begin{bmatrix} 1-\Upsilon & R-\chi \\ -1 & 0 \end{bmatrix}, & \chi^{max} - \chi > 0 \\ \\ M_2 := \begin{bmatrix} 1-\Upsilon & R-\chi \\ 0 & 1 \end{bmatrix}, & \Upsilon > 0 \end{cases} . \tag{4.7}$$

From (4.7) we can further compute its Bouligand subdifferential as the set $\partial_B H := \{M_1, M_2\}$ and its convex hull, the Clarke's generalized Jacobian $\partial H$,

$$\partial H := \{ \begin{bmatrix} 1-\Upsilon & R-\chi \\ \alpha & \alpha+1 \end{bmatrix}, -1 \leq \alpha \leq 0 \}.$$

We find then that any selection $M$ from $\partial H$, thanks to $R >> \chi_j^n$ and $\Upsilon_j^n < 1$, is always positive definite thus nonsingular. Thus, from [134], Prop. 2.12, we conclude that the Newton's method converges q-superlinearly.

Now consider the implicit treatment of diffusion, i.e., $\bar{n} = n$. At each time step $n$ we have to solve a system of nonlinear equations with $2 \times M$ unknowns, where $M$ is the number of spatial discretization points. Jacobian of that system is sparse and its blocks resemble $H'$ in (4.6) because the constraints (4.5) have to hold at every point $j, n$. The properties of that system follow from analyses similar to that for $\bar{n} = n - 1$.

**4.3. Remarks on the full model.** Thanks to several simplifying assumptions concerning $P, T, \chi_{lS}$ we derived (2.7) for which our discussions in Sections 4.1 and 4.2 lead to the insight into the main difficulties of numerical hydrate modeling. These model simplifications must be removed for realistic simulations, and (2.7) must be complemented by an energy equation including the latent heat of phase transition. Furthermore, gas, hydrate, and brine phase compressibilities, as well as the dependence of transport properties upon the primary variables, need to be accounted for. In addition, gas phase mobility and fluxes, also through hydrate zone, cannot be ignored; in fact, capillary pressure needs to be included in the model, since from the observations of hydrates in subsea sediments it is known that the methane bubbles percolate the hydrate zone through various free gas conduits.

The comprehensive models described in [76, 48, 101, 80, 29, 87, 132] are quite general and account for most of these dynamic effects using available experimental data and, when the experimental data is missing, using some heuristic relationships. For example, a model of hydrate evolution should account in some way for the hydrate growth in pore space, and most models [48, 76] do so via heuristic relationships such as $\phi = \phi(S_h)$, $K = K(S_h)$, which are unsupported by experiments or first principles models. The full mesoscale models for hydrate evolution are therefore lacking precision due to the lack of qualitative and quantitative information on the dynamics

of hydrate formation and dissociation and its effects on porescale. See Section 5 for a discussion of qualitative and quantitative model elements following from porescale studies.

**5. Porescale modeling.** In Sections 2-4 we discussed the need for accurate models of dynamics of certain phenomena in ECBM and MH which are unavailable or hard to obtain experimentally. In ECBM models it is important to model porescale changes to the coal matrix under adsorption due to swelling [90, 91]. However, there is virtually no experimental work on porescale; this can be partially explained by the softness of coal and the difficulty to obtain rock coal samples other than those made from pulverized coal. For MH, we are interested in phase transitions associated with hydrate formation and dissociation, a phenomenon not yet entirely understood, see [127], Chapters 3-5. It is known that it proceeds in several steps, one of which includes the (Langmuir) adsorption of gas particles into the water structure surrounding the trapped gas molecules. The hydrate formation process includes heat and mass transfer, and metastable states, while dissociation is an endothermic process because heat must be supplied to break the bonds between guest and water molecules and the hydrogen bonds between water molecules. Finally, there is substantial permeability decrease due to the presence of hydrate [88, 29, 76]; there are ongoing porescale imaging efforts [3, 117] which show that the models depend on the type of sediment and processes. However, experiments are difficult due to the instability of hydrates in standard conditions. In related work, [61] discusses the dependence between capillary invasion and fracture opening parametrized by grain size; however, changes in the geometry due to the transport of dissolved methane and/or hydrate formation are not accounted for. We argue that the nonlinear relationships necessary for ECBM and MH can be obtained from porescale computational models which can provide a virtual laboratory for much of the detailed data.

Until about a decade ago, most modeling in porous media relied on continuum models at mesoscale, carrying the quantitative information upwards to reservoir scale by upscaling or multiscale modeling. There exist now various pore network [73, 74, 8, 18], Lattice-Boltzmann methods [141, 128, 121, 139], as well as continuum-based models [108, 103, 102] which simulate processes at porescale and supply data for the meso-scale models, or support them qualitatively (our references are rather incomplete due to lack of space). Other discrete methods based on so-called first principles have been successful in various disciplines and these include molecular dynamics (MD), density functional theory (DFT), and various Monte Carlo techniques, see [9, 113, 54, 146, 69]. More generally, statistical mechanics offers an approach in which "deterministic equations describing (large systems of) particles are replaced by assumptions on their statistical behavior" [19]. Particularly relevant for ECBM and MH are equilibrium lattice gas models and specifically, those based on mean field theory

(MFEQ) [22, 130, 92]. Below we outline possible directions for ECBM and MH tied to some of our current work on porescale.

**5.1. Porescale models of $\phi, K$.** Let the porespace $\omega = \omega_R \cup \omega_F = \bigcup_{i=1}^N \omega_i$ be a collection of rectangular cells (sites) $\omega_i$, with random variables $\mathbf{t}, \mathbf{n}$ denoting matrix (rock) and fluid occupation variables; see Figure 6 for illustration. The geometry of $\omega$ whose comes either directly from tomography and X-ray analyses, or is constructed synthetically based on some heuristics or on experimental structure factors such as mean, percolation, and two-point correlations. Note that $\mathbf{t}$ is usually called *a (quenched) disorder*. At a site $i$,

$$t_i = \begin{cases} 1, & \text{cell is open to fluid} \\ 0, & \text{cell is blocked by solid} \end{cases} \tag{5.1}$$

$$n_i = \begin{cases} 1, & \text{cell is occupied by fluid} \\ 0, & \text{cell is not occupied by fluid} \end{cases} \tag{5.2}$$

We have $\omega_F := \bigcup_{i:t_i=1} \omega_i$ and we will denote $|\omega_F| := \sum_i t_i$ with the porosity given by $\phi = \frac{|\omega_F|}{|\omega_F|+|\omega_R|} = \frac{N_F}{N}$. Also, the rock-fluid interface is denoted by $\gamma := \partial\omega_F \cap \partial\omega_R$. In discrete models only $t_i, n_i$ are important; the continuum models are posed with respect to a position variable $y \in \omega_F$.

Let $\phi$ and $K$ respond dynamically to the formation stress and to the presence of hydrates, adsorption in the matrix, and other phenomena, which we write as

$$K = g(\phi; \xi), \tag{5.3}$$

where $\xi$ is a model-dependent collection of variables.

Now let $\phi_0, K_0$ be some reference values of $\phi, K$; assume for simplicity that $K$ is isotropic. In ECBM the formula $\frac{K}{K_0} = (\frac{\phi}{\phi_0})^3$ for (5.3) or its generalizations have been used in [91, 83] but these do not account for the coal matrix swelling. For MH, $\phi = \phi_0(1 - S_h)$ shows the porosity changes due to the hydrate presence via its saturation $S_h$, and $K = K_0(1 - S_h)^2$ for the *pore coating* models, or, via a more rapidly decaying relationship, $K = K_0(1 - S_h^2 + \frac{2(1-S_h)^2}{\log(S_h)})$ for the *pore filling* models [29, 76, 88]. These expressions are based on conceptual models of porous media as a bundle of capillaries, i.e., Carman-Kozeny [17, 67] formula $K = \phi\frac{d_g^2}{12}$, where $d_g$ is the grain size. These models and correlations, while valuable in simple circumstances, lack the precision for complex multicomponent phenomena.

A computational model to derive (5.3) starts with a given porescale geometry $\omega$ and a given $\xi$, and solves fluid flow equations whose solutions we can then average to obtain (5.3). For an evolving $\xi$ we need to solve as well the diffusive and advective transport models governing $\xi$ at porescale; see an illustration in Figure 6. In particular, for ECBM and MH these need to account for adsorption and phase transition, respectively. A prevailing

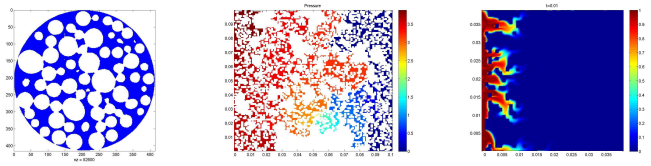

FIG. 6. *Left: example of disorders* $\mathbf{t}$ *from porescale data from [109], courtesy of Dorthe Wildenschild (OSU). Middle and right: flow and transport simulations at porescale, in collaboration with Anna Trykozko (ICM UW)*

number of computational models of adsorption and phase transitions at porescale are discrete. However, some models [72, 116], allow the treatment of adsorption as a surface reaction modeled by a boundary condition of Robin- or Neumann type posed on $\gamma$. These have shown to be most compatible in our studies thus far, while the discrete models appear to be better for providing models for the dynamics of the phenomena such as those in (2.6), discussed next.

**5.2. Adsorption and phase transitions at porescale.** The nonlinear relationships such as (3.3) or, more generally, (2.6), governing the dynamics of adsorption and phase transitions are usually known experimentally for some range of parameters and components. Precise quantitative models for any set of parameters and any number of components are needed for the computational simulations, and ultimately for better understanding of the phenomena relevant for ECBM and MH at pore- and mesoscale. As mentioned above, we have had some preliminary success with the discrete rather than continuum models at porescale in this regard.

Specifically, the MFEQ theory accounts for the particles of fluid interacting with each other and adsorbing on the porous matrix and/or undergoing phase transitions. These interactions are expressed by a Hamiltonian, i.e., an energy functional with various product terms which are simplified in the mean field approximation. There are successful MFEQ models for adsorption and phase transitions developed in [64] based on the Ising model [92, 68]; they have been refined and compared to other methods in [63, 142, 143, 120, 53, 85, 118, 119]. For $N_R = N - N_F >> 1$, there are several metastable equilibria in the Ising model [92, 37], and this leads to adsorption/desorption hysteresis and irreversibility of phase transition.

The MFEQ models for adsorption were derived and validated for single-component adsorbate in mesoporous glasses. We are working on extending them to multiple components in micropores and macropores in the sediments and coals; these models will provide the porescale counterparts of IAS-Langumir models from Section 3.4 and those with memory in Section 3.2. Another modification accounts for the swelling of the matrix which is directly linked to the adsorption. Next, the discrete models of adsorption given by MFEQ provide scanning curves for adsorption-desorption

hysteresis at arbitrary reversal points, and they have advantages over the models derived from experiments or the differential models described in Section 3.3 since they are easily extended to multiple components.

As concerns the phase transitions, the mean field approximation is capable of producing some good qualitative approximations to phase transitions and critical phenomena [146, 92]. We are working on a simple model of hydrate formation analogous to MFEQ models for adsorption. Compared to the classical Ising model of phase transition, it is defined in porespace, and its Hamiltonian can be formulated so as to promote either pore coating or filling.

**5.3. Hybrid models: connection between porescale and meso--scale models.** The exposition above argues for implementation of porescale models to provide missing data for mesoscale simulations. One needs to consider several fundamental issues directly determining their usefulness.

First concerns the choice of porescale models. The discrete and stochastic models at porescale are fairly easy to implement, but are typically very computationally expensive and their interpretation is hard. On the other hand, continuum models at porescale and mesoscale require deep understanding in the start-up phase but the interpretation of the simulation results is fairly standard.

Second issue concerns the qualitative properties of their solutions. Once the porescale models are implemented, we should show, e.g., that the isotherms provided by MFEQ calculations have indeed the qualitative mathematical properties expected of the isotherms. An analogous issue concerns other results of porescale simulations.

The last but not the least issue is that of computational complexity. The common feature of the various porescale models is their large demand on the computational time which increases with $|\omega|$; the latter is as large as possible since $\omega$ is intended to be a Representative Elementary Volume (REV). In addition, we (may) need to consider several statistical realizations of the REVs. This combined computational complexity has precluded dynamic connections between porescale and mesoscale so far, while the mesoscale models are the only ones that can be used in optimization loops, reservoir characterization, parameter identification, and control.

We believe it is possible for some of our porescale results to be encapsulated as library entries similar to the lookup tables, with properties similar to the traditional heuristic models. As concerns the complexity, coarse grained discrete models coupled to continuum models have been successful in other fields [40, 89, 84, 58]. Also, some porescale models can be perhaps implemented efficiently on modern computer architectures such as multicore or graphic processing units. However, there are yet no universal ways to overcome the computational complexity of the hybrid models.

**6. Summary and acknowledgements.** In this paper we have presented a collection of comprehensive and simplified models for ECBM and

MH at mesoscale and underlined the main difficulties in their numerical approximation. Furthermore, we indicated the need for detailed dynamics information for some of the processes and proposed to use porescale computations to derive these. We believe that some porescale models based on coarse graining, and a careful choice of REVs and their samples, can lead to dynamic hybrid models combining porescale and mesoscale models which can be very useful for the needs of MH and ECBM modeling.

Research in this paper has been partially supported by various sources, and benefited from discussions with several colleagues We thank the IMA for hosting the author at the workshops in May 2009, October 2011 and as a short-term visitor in Spring 2011. We also thank Interdisciplinary Centre for Modeling at the University of Warsaw (ICM UW), where the author was a Fulbright Research scholar in 2009-2010. Much of our knowledge on the discrete models came from these visits. To Professor Knabner we owe the insight into semi-smooth Newton methods; we are also grateful to Professors Ben-Gharbia and Jaffre from INRIA for sharing more information on this topic. We also thank Professor Showalter (OSU) for many discussions on monotone operators over the years. Our understanding of continuum models of ECBM and MH benefitted substantially from discussions with Professors Ceglarska-Stefańska and Czerw (University of Mining and Metalurgy, Cracow, Poland), and Professors Trèhu and Torres (COAS at OSU), respectively. Our collaborators Professors Wildenschild (OSU) and Trykozko (ICM UW) provided data for images in Figure 6.

## REFERENCES

[1] IUPAC, International Union of Pure and Applied Chemistry `http://www.iupac.org/`.

[2] Stomp: Subsurface Transport Over Multiple Phases simulator website `http://stomp.pnl.gov/`, note = "[online; accessed 11-january-2010]".

[3] The National Methane Hydrates R&D Program, `http://www.netl.doe.gov/technologies/oil-gas/FutureSupply/MethaneHydrates/maincontent.htm`,.

[4] TOUGH Family of Codes: Availability and Licensing, `http://esd.lbl.gov/TOUGH2/avail.html`. [Online; accessed 11-January-2010].

[5] Ocean Observatories Initiative, `http://www.oceanleadership.org/programs-and-partnerships/ocean-observing/ooi/`, 2007.

[6] Sea expedition studies off the coast of northern Alaska, `http://www.netl.doe.gov/publications/press/2009/09075-Beaufort_Sea_Expedition_Studies_Me.html`, September 2009. NETL, U.S. Naval Research Laboratory and Royal Netherlands Institute for Sea Research, [Online; accessed 12-January-2010].

[7] Neptune Canada, `http://neptunecanada.ca/about-neptune-canada/neptune-canada-101.dot`,, 2010.

[8] David Adalsteinsson and Markus Hilpert. Accurate and efficient implementation of pore-morphology-based drainage modeling in two-dimensional porous media. *Transp. Porous Media*, 65(2):337–358, 2006.

[9] M.P. Allen and D.J. Tildesley. *Computer Simulation of Liquids*. Oxford Science Publishers, 1987.

[10] H. W. Alt and E. di Benedetto. Nonsteady flow of water and oil through in-

homogeneous porous media. *Ann. Scuola Norm. Sup. Pisa Cl. Sci. (4)*, 12(3):335–392, 1985.

[11] T. Arbogast. The existence of weak solutions to single porosity and simple dual-porosity models of two-phase incompressible flow. *Nonlinear Analysis, Theory, Methods and Applications*, 19:1009–1031, 1992.

[12] Todd Arbogast, Jim Douglas, Jr., and Ulrich Hornung. Derivation of the double porosity model of single phase flow via homogenization theory. *SIAM J. Math. Anal.*, 21(4):823–836, 1990.

[13] P. C. Ball and R. Evans. Temperature dependence of gas adsorption on a mesoporous solid: capillary criticality and hysteresis. *Langmuir*, 5(3):714–723, 1989.

[14] J. W. Barrett, H. Kappmeier, and P. Knabner. Lagrange-Galerkin approximation for advection-dominated contaminant transport with nonlinear equilibrium or non-equilibrium adsorption. In *Modeling and computation in environmental sciences (Stuttgart, 1995)*, volume 59 of *Notes Numer. Fluid Mech.*, pages 36–48. Vieweg, Braunschweig, 1997.

[15] John W. Barrett and Peter Knabner. Finite element approximation of the transport of reactive solutes in porous media. II. Error estimates for equilibrium adsorption processes. *SIAM J. Numer. Anal.*, 34(2):455–479, 1997.

[16] John W. Barrett and Peter Knabner. An improved error bound for a Lagrange-Galerkin method for contaminant transport with non-Lipschitzian adsorption kinetics. *SIAM J. Numer. Anal.*, 35(5):1862–1882 (electronic), 1998.

[17] Jacob Bear. *Dynamics of Fluids in Porous Media*. Dover, New York, 1972.

[18] Martin Blunt. Flow in porous media pore-network models and multiphase flow. *Current Opinion in Colloid & Interface Science*, 6:197–207, 2001.

[19] Oliver Bühler. *A brief introduction to classical, statistical, and quantum mechanics*, volume 13 of *Courant Lecture Notes in Mathematics*. New York University Courant Institute of Mathematical Sciences, New York, 2006.

[20] Andreas Busch, Yves Gensterblum, Bernhard M. Krooss, and Ralf Littke. Methane and carbon dioxide adsorption-diffusion experiments on coal: upscaling and modeling. *International Journal of Coal Geology*, 60(2-4):151 – 168, 2004.

[21] Andreas Busch, Yves Gensterblum, Bernhard M. Krooss, and Nikolai Siemons. Investigation of high-pressure selective adsorption/desorption behaviour of co2 and CH4 on coals: An experimental study. *International Journal of Coal Geology*, 66(1-2):53 – 68, 2006.

[22] Herbert B. Callen. *Thermodynamics, an introduction to physical theories of equilibrium thermostatics amd irreversible thermodynamics*. Wiley, 1960.

[23] Grazyna Ceglarska-Stefanska and Katarzyna Zarebska. The competitive sorption of CO2 and CH4 with regard to the release of methane from coal. *Fuel Processing Technology*, 77-78:423 – 429, 2002.

[24] Grazyna Ceglarska-Stefanska and Katarzyna Zarebska. Sorption of carbon dioxide-methane mixtures. *International Journal of Coal Geology*, 62(4):211 – 222, 2005.

[25] Zhangxin Chen, Guan Qin, and Richard E. Ewing. Analysis of a compositional model for fluid flow in porous media. *SIAM J. Appl. Math.*, 60(3):747–777 (electronic), 2000.

[26] C. R. Clarkson and R. M. Bustin. The effect of pore structure and gas pressure upon the transport properties of coal: a laboratory and modeling study. 1. isotherms and pore volume distributions. *Fuel*, 78(11):1333 – 1344, 1999.

[27] C. R. Clarkson and R. M. Bustin. The effect of pore structure and gas pressure upon the transport properties of coal: a laboratory and modeling study. 2. adsorption rate modeling. *Fuel*, 78(11):1345 – 1362, 1999.

[28] H. Class, R. Helmig, and P. Bastian. Numerical simulation of non-isothermal ultiphase multicomponent processes in porous media 1. an efficient solution technique. *Advances in Water Resources*, 25:533–550, 2002.

[29] M. B. Clennell, M. Hovland, J.S. Booth, P. Henry, and W. Winters. Formation of natural gas hydrates in marine sediments 1. conceptual model of gas hydrate growth conditioned by host sediment properties. *Journal of Geophysical Research*, 104:22,985–23,003, 1999.

[30] B. Cockburn, G. Gripenberg, and S.-O. Londen. On convergence to entropy solutions of a single conservation law. *J. Differential Equations*, 128(1):206–251, 1996.

[31] L.D. Connell and C. Detournay. Coupled flow and geomechanical processes during enhanced coal seam methane recovery through CO2 sequestration. *International Journal of Coal Geology*, 77(1-2):222 – 233, 2009. CO2 Sequestration in Coals and Enhanced Coalbed Methane Recovery.

[32] Richard W. Cottle, Jong-Shi Pang, and Richard E. Stone. *The linear complementarity problem*. SIAM, 2009.

[33] M.K. Davie and B. A. Buffett. A numerical model for the formation of gas hydrates below the seafloor. *Journal of Geophysical Research*, 106(B1):497–514, 2001.

[34] M.K. Davie and B. A. Buffett. A steady state model for marine hydrate formation: Constraints on methane supply from pore water sulfate profiles. *Journal of Geophysical Research*, 108:B10, 2495, 2003.

[35] C. N. Dawson. Godunov-mixed methods for advection-diffusion equations in multidimensions. *SIAM J. Numer. Anal.*, 30:1315–1332, 1993.

[36] C. N. Dawson, C. J. van Duijn, and M. F. Wheeler. Characteristic-Galerkin methods for contaminant transport with nonequilibrium adsorption kinetics. *SIAM J. Numer. Anal.*, 31(4):982–999, 1994.

[37] Pablo G. Debenedetti. *Metastable liquids. concepts and principles*. Princeton University Press, 1996.

[38] G. R. Dickens. Rethinking the global carbon cycle with a large, dynamic and microbially mediated gas hydrate capacitor. *Earth Planet. Sci. Lett.*, 213, 2003.

[39] Duong D. Do. *Adsorption analysis: equilibria and kinetics*. Imperial College Press, 1998.

[40] Matthew Dobson and Mitchell Luskin. An optimal order error analysis of the one-dimensional quasicontinuum approximation. *SIAM J. Numer. Anal.*, 47(4):2455–2475, 2009.

[41] J. Douglas, Jr., M. Peszyńska, and R. E. Showalter. Single phase flow in partially fissured media. *Transp. Porous Media*, 28:285–306, 1997.

[42] Z. Duan. GEOCHEM_ORG website `http://www.geochem-model.org`. [Online; accessed 28-December-2009].

[43] Z. Duan and S. Mao. A thermodynamic model for calculating methane solubility, density and gas phase composition of methane-bearing aqueous fluids from 273 to 523 k and from 1 to 2000 bar. *Geochimica et Cosmochimica Acta*, 70:3369–3386, 2006.

[44] D.H. Everett. In D. H. Everett and F. S. Stone, editors, *The Structure and Properties of Porous Materials*. Butterworths, London, 1958.

[45] R.W. Falta, K. Pruess, I. Javandel, and P. A Witherspoon. Numerical modeling of steam injection for the removal of nonaqueous phase liquids from the subsurface 1. numerical formulation. *Water Res. Research*, 28(2):433–449, 1992.

[46] Masaji Fujioka, Shinji Yamaguchi, and Masao Nako. CO2-ECBM field tests in the ishikari coal basin of japan. *International Journal of Coal Geology*, 82(3-4):287 – 298, 2010. Asia Pacific Coalbed Methane Symposium: Selected papers from the 2008 Brisbane symposium on coalbed methane and CO2-enhanced coalbed methane.

[47] T. S. Collett G. J. Moridis, S. R. Dallimore, T. Satoh, S. Hancock, and B. Weatherill. Numerical studies of gas production from several $ch_4$-hydrate zones at the Mallik site, Mackenzie Delta, Canada. Technical report.

[48] S.K. Garg, J.W. Pritchett, A. Katoh, K. Baba, and T. Fijii. A mathematical model for the formation and dossociation of methane hydrates in the marine environment. *Journal of Geophysical Research*, 113:B08201, 2008.

[49] Y. Gensterblum, P. van Hemert, P. Billemont, E. Battistutta, A. Busch, B.M. Krooss, G. De Weireld, and K.-H.A.A. Wolf. European inter-laboratory comparison of high pressure CO2 sorption isotherms ii: Natural coals. *International Journal of Coal Geology*, 84(2):115 – 124, 2010.

[50] I. Ben Gharbia and J. Jaffre. Gas phase appearance and disappearance as a problem with complementarity constraints. Technical Report 7803, INRIA Research Report, November 2011.

[51] A.L. Goodman, A. Busch, R.M. Bustin, L. Chikatamarla, S. Day, G.J. Duffy, J.E. Fitzgerald, K.A.M. Gasem, Y. Gensterblum, C. Hartman, C. Jing, B.M. Krooss, S. Mohammed, T. Pratt, R.L. Robinson Jr., V. Romanov, R. Sakurovs, K. Schroeder, and C.M. White. Inter-laboratory comparison ii: CO2 isotherms measured on moisture-equilibrated argonne premium coals at 55c and up to 15mpa. *International Journal of Coal Geology*, 72(3-4):153 – 164, 2007.

[52] G. Gripenberg. Nonsmoothing in a single conservation law with memory. *Electron. J. Differential Equations*, pages No. 8, 8 pp. (electronic), 2001.

[53] P.A. Monson H.-J. Woo, L. Sarkisov. Understanding adsorption hysteresis in porous glasses and other mesoporous materials. In *Characterization of porous solids VI ; Studies in surface science and catalysis*, volume 144. 2002.

[54] J. M. Haile. *Molecular Dynamics Simulation*. Wiley, 1997.

[55] Satya Harpalani, Basanta K. Prusty, and Pratik Dutta. Methane/CO2 sorption modeling for coalbed methane production and CO2 sequestration. *Energy & Fuels*, 20(4):1591–1599, 2006.

[56] R. Helmig. *Multiphase flow and transport processes in the Subsurface*. Springer, 1997.

[57] P. Henry, M. Thomas, and M. B. Clennell. Formation of natural gas hydrates in marine sediments 2. Thermodynamic calculations of stability conditions in porous sediments. *Journal of Geophysical Research*, 104:23,005–23,022, 1999.

[58] Desmond J. Higham. Modeling and simulating chemical reactions. *SIAM Rev.*, 50(2):347–368, 2008.

[59] Ulrich Hornung and Ralph E. Showalter. Diffusion models for fractured media. *J. Math. Anal. Appl.*, 147(1):69–80, 1990.

[60] Kazufumi Ito and Karl Kunisch. *Lagrange multiplier approach to variational problems and applications*, volume 15 of *Advances in Design and Control*. Society for Industrial and Applied Mathematics (SIAM), Philadelphia, PA, 2008.

[61] A.K. Jain and R. Juanes. Preferential mode of gas invasion in sediments: Grain scale mechanistic model of coupled multiphase fluid flow and sediment mechanics. *Journal of Geophysical Research*, 114:B08101, 2009.

[62] Kristian Jessen, Wenjuan Lin, and Anthony R. Kovscek. Multicomponent sorption modeling in ECBM displacement calculations. *SPE 110258*, 2007.

[63] E. Kierlik, P. A. Monson, M. L. Rosinberg, L. Sarkisov, and G. Tarjus. Capillary condensation in disordered porous materials: Hysteresis versus equilibrium behavior. *Phys. Rev. Lett.*, 87(5):055701, Jul 2001.

[64] E. Kierlik, M.L. Rosinberg, G. Tarjus, and E. Pitard. Mean-spherical approximation for a lattice model of a fluid in a disordered matrix. *Molecular Physics: An International Journal at the Interface Between Chemistry and Physics*, 95:341–351, 1998.

[65] G. R. King, T. Ertekin, and F. C. Schwerer. Numerical simulation of the transient behavior of coal-seam degasification wells. *SPE Formation Evaluation*, 2:165–183, April 1986.

[66] Viviane Klein and Małgorzata Peszyńska. Adaptive multi-level modeling of cou-

pled multiscale phenomena with applications to methane evolution in subsurface. In *Proceedings of CMWR XVIII in Barcelona, June 21-24, 2010*. available online at http://congress.cimne.com/CMWR2010/Proceedings, 2010. paper 47.

[67] L. W. Lake. *Enhanced oil recovery*. Prentice Hall, 1989.

[68] David Lancaster, Enzo Marinari, and Giorgio Parisi. Weighted mean-field theory for the random field Ising model. *J. Phys. A*, 28(14):3959–3973, 1995.

[69] D.P. Landau and K. Binder. *A Guide to Monte-Carlo Simulations in Statistical Physics*. Cambridge, 2000.

[70] R.J. Lenhard, M. Oostrom, and M.D. White. Modeling fluid flow and transport in variably saturated porous media with the STOMP simulator. 2. Verification and validation exercises. *Advances in Water Resources*, 18(6), 1995.

[71] Randall J. LeVeque. *Numerical methods for conservation laws*. Lectures in Mathematics ETH Zürich. Birkhäuser Verlag, Basel, 1990.

[72] J. Lewandowska, A. Szymkiewicz, K. Burzynski, and M. Vauclin. Modeling of unsaturated water flow in double-porosity soils by the homogenization approach. *Advances in Water Resources*, 27:283–296, 2004.

[73] Li Li, Catherine A. Peters, and Michael A. Celia. Upscaling geochemical reaction rates using pore-scale network modeling. *Advances in Water Resources*, 29(9):1351 – 1370, 2006.

[74] W. Brent Lindquist. Network flow model studies and 3D pore structure. In *Fluid flow and transport in porous media: mathematical and numerical treatment (South Hadley, MA, 2001)*, volume 295 of *Contemp. Math.*, pages 355–366. Amer. Math. Soc., Providence, RI, 2002.

[75] X. Liu and P. B. Flemings. Passing gas through the hydrate stability zone at southern hhydrate ridge, offshore oregon. *EPSL*, 241:211–226, 2006.

[76] X. Liu and P. B. Flemings. Dynamic multiphase flow model of hydrate formation in marine sediments. *Journal of Geophysical Research*, 112:B03101, 2008.

[77] Q. Lu, M. Peszyńska, and M. F. Wheeler. A parallel multi-block black-oil model in multi-model implementation. *SPE Journal*, 7(3):278–287, September 2002. SPE 79535.

[78] Zofia Majewska, Grazyna Ceglarska-Stefanska, Stanislaw Majewski, and Jerzy Zietek. Binary gas sorption/desorption experiments on a bituminous coal: Simultaneous measurements on sorption kinetics, volumetric strain and acoustic emission. *International Journal of Coal Geology*, 77(1-2):90 – 102, 2009. CO2 Sequestration in Coals and Enhanced Coalbed Methane Recovery.

[79] A. Malinverno, M. Kastner, M.E. Torres, and U.G. Wortmann. Gas hydrate occurence from pore water chlorinity and downhhole logs in a transect across the northern cascadia margin (integrated ocean drilling program expediction 311. *Journal of Geophysical Research*, 113:B08103, 2008.

[80] K. Masataka, N. Yukihiko, G. Shusaku, and A. Juichiro. Effect of the latent heat on the gas–hydrate/gas phase boundary depth due to faulting. *Bulletin of Earthquake Research Institute, University of Tokyo*, 73, 1998.

[81] P. Massarotto, S.D. Golding, J.-S. Bae, R. Iyer, and V. Rudolph. Changes in reservoir properties from injection of supercritical CO2 into coal seams – a laboratory study. *International Journal of Coal Geology*, 82(3-4):269 – 279, 2010. Asia Pacific Coalbed Methane Symposium: Selected papers from the 2008 Brisbane symposium on coalbed methane and CO2-enhanced coalbed methane.

[82] S. Mazumder, K. Wolf, P. van Hemert, and A. Busch. Laboratory experiments on environmental friendly means to improve coalbed methane production by carbon dioxide/flue gas injection. *Transport in Porous Media*, 75:63–92, 2008. 10.1007/s11242-008-9222-z.

[83] Saikat Mazumder and Karl Heinz Wolf. Differential swelling and permeability change of coal in response to CO2 injection for ECBM. *International Journal of Coal Geology*, 74(2):123 – 138, 2008.

[84] N. Moes, J. T. Oden, and K. Vemaganti. A two-scale strategy and a posteriori error estimation for modeling heterogeneous structures. In *On new advances in adaptive computational methods in mechanics*. Elsevier, 1998.

[85] Peter Monson. Recent progress in molecular modeling of adsorption and hysteresis in mesoporous materials. *Adsorption*, 11:29–35(7), July 2005.

[86] G.J. Moridis, T. Collett, S.R. Dallimore, T. Satoh, S. Hancock, and B. Weatherhill. Numerical studies of gas production from several $ch_4$-hydrate zones at the Mallik site, mackenzie delta, candada. Technical report, LBNL-50257, 2002.

[87] Kambiz Nazridoust and Goodarz Ahmadi. Computational modeling of methane hydrate dissociation in a sandstone core. *Chemical Engineering Science*, 62(22):6155 – 6177, 2007.

[88] J. Nimblett and C. Ruppel. Permeability evolution during the formation of gas hydratees in marine sediments. *Journal of Geophysical Research*, 108:B9, 2420, 2003.

[89] Christoph Ortner and Endre Süli. Analysis of a quasicontinuum method in one dimension. *M2AN Math. Model. Numer. Anal.*, 42(1):57–91, 2008.

[90] Zhejun Pan and Luke D. Connell. A theoretical model for gas adsorption-induced coal swelling. *International Journal of Coal Geology*, 69(4):243 – 252, 2007.

[91] Zhejun Pan, Luke D. Connell, and Michael Camilleri. Laboratory characterisation of coal reservoir permeability for primary and enhanced coalbed methane recovery. *International Journal of Coal Geology*, 82(3-4):252 – 261, 2010. Asia Pacific Coalbed Methane Symposium: Selected papers from the 2008 Brisbane symposium on coalbed methane and CO2-enhanced coalbed methane.

[92] Giorgio Parisi. *Statistical Field Theory*. Addison-Wesley, 1988.

[93] M. Peszynska. Numerical model for adsorption hysteresis. manuscript.

[94] M. Peszynska. Numerical scheme for a scalar conservation law with memory. submitted.

[95] M. Peszyńska. Finite element approximation of a model of nonisothermal flow through fissured media. In R. Stenberg M. Krizek, P. Neittaanmaki, editor, *Finite Element Methods*, Lecture Notes in Pure and Applied Mathematics, pages 357–366. Marcel Dekker, 1994.

[96] M. Peszyńska. A differential model of adsorption hysteresis with applications to chromatography. In Jorge Guinez Angel Domingo Rueda, editor, *III Coloquio sobre Ecuaciones Diferenciales Y Aplicaciones, May 1997*, volume II. Universidad del Zulia, 1998.

[97] M. Peszyńska. The total compressibility condition and resolution of local nonlinearities in an implicit black-oil model with capillary effects. *Transport in Porous Media*, 63(1):201 – 222, April 2006.

[98] M. Peszyńska and R. E. Showalter. A transport model with adsorption hysteresis. *Differential Integral Equations*, 11(2):327–340, 1998.

[99] M. Peszyńska and R. E. Showalter. Multiscale elliptic-parabolic systems for flow and transport. *Electron. J. Diff. Equations*, 2007:No. 147, 30 pp. (electronic), 2007.

[100] M. Peszynska, R.E. Showalter, and S.-Y.Yi. Homogenization of a pseudoparabolic system. *Applicable Analysis*, 88(9):1265–1282, 2009.

[101] M. Peszyńska, M. Torres, and A. Tréhu. Adaptive modeling of methane hydrates. In *International Conference on Computational Science, ICCS 2010, Procedia Computer Science, available online via www.elsevier.com/locate/procedia and www.sciencdirect.com*, volume 1, pages 709–717, 2010.

[102] M. Peszyńska and A. Trykozko. Convergence and stability in upscaling of flow with inertia from porescale to mesoscale. *International Journal for Multiscale Computational Engineering*, 9(2):215–229, 2011.

[103] M. Peszyńska, A. Trykozko, and W. Sobieski. Forchheimer law in computational and experimental studies of flow through porous media at porescale and mesoscale. In *Mathematical Sciences and Applications*, volume 32 of

*Current Advances in Nonlinear Analysis and Related Topics*, pages 463–482. GAKUTO Internat. Ser. Math. Sci. Appl., 2010.

[104] M. Peszyńska, M. F. Wheeler, and I. Yotov. Mortar upscaling for multiphase flow in porous media. *Computational Geosciences*, 6:73–100, 2002.

[105] Małgorzata Peszyńska. Analysis of an integro-differential equation arising from modelling of flows with fading memory through fissured media. *J. Partial Differential Equations*, 8(2):159–173, 1995.

[106] Małgorzata Peszyńska. On a model of nonisothermal flow through fissured media. *Differential Integral Equations*, 8(6):1497–1516, 1995.

[107] Małgorzata Peszyńska. Finite element approximation of diffusion equations with convolution terms. *Math. Comp.*, 65(215):1019–1037, 1996.

[108] Malgorzata Peszynska, Anna Trykozko, and Kyle Augustson. Computational upscaling of inertia effects from porescale to mesoscale. In G. Allen, J. Nabrzyski, E. Seidel, D. van Albada, J. Dongarra, and P. Sloot, editors, *ICCS 2009 Proceedings, LNCS 5544, Part I*, pages 695–704, Berlin-Heidelberg, 2009. Springer-Verlag.

[109] Mark L. Porter, Marcel G. Schaap, and Dorthe Wildenschild. Lattice-Boltzmann simulations of the capillary pressure-saturation-interfacial area relationship for porous media. *Advances in Water Resources*, 32(11):1632 – 1640, 2009.

[110] K. Pruess. TOUGH2 – a general-purpose numerical simulator for multiphase fluid andheat flow. Technical Report LBL 29400, Lawrence Berkeley Laboratory, University of California, Berkeley, Calif, 1991.

[111] Karsten Pruess and Julio Garcia. Multiphase flow dynamics during CO2 disposal into saline aquifers. *Environmental Geology*, 42:282–295, 2002.

[112] Basanta Kumar Prusty. Sorption of methane and CO2 for enhanced coalbed methane recovery and carbon dioxide sequestration. *Journal of Natural Gas Chemistry*, 17(1):29 – 38, 2008.

[113] D.C. Rapaport. *The art of molecular dynamics simulation*. Cambridge, 4 edition, 2009.

[114] E. Ruckenstein, A. S. Vaidyanathan, and G.R. Youngquist. Sorption by solids with bidisperse pore structures. *Chemical Engrg. Science*, 26:1305–1318, 1971.

[115] W. Rudzinski and D.H. D. H. Everett. *Adsorption of gases on heterogeneous surfaces*. Academic Press, 1992.

[116] Emily M. Ryan, Alexandre M. Tartakovsky, and Cristina Amon. Investigating the accuracy of a darcy scale model of competitive adsorption in a porous medium through sph pore scale modeling. In *Proceedings of CMWR XVIII in Barcelona, June 21-24, 2010*. available online at http://congress.cimne.com/CMWR2010/Proceedings, 2010. paper 94.

[117] Marisa B. Rydzy, Mike L. Batzle, Keith C. Hester, Jim Stevens, and James J. Howard. Rock physics characterization of hydrate-bearing ottawa sand f110. In *DHI/Fluid Consortium Meeting Fall 2010*, 2010.

[118] L. Sarkisov and P. A. Monson. Computer simulations of phase equilibrium for a fluid confined in a disordered porous structure. *Phys. Rev. E*, 61(6):7231–7234, Jun 2000.

[119] L. Sarkisov and P. A. Monson. Modeling of adsorption and desorption in pores of simple geometry using molecular dynamics. *Langmuir*, 17(24):7600–7604, 2001.

[120] L. Sarkisov and P. A. Monson. Lattice model of adsorption in disordered porous materials: Mean-field density functional theory and Monte Carlo simulations. *Physical Review E (Statistical, Nonlinear, and Soft Matter Physics)*, 65(1):011202, 2002.

[121] M.G. Schaap, M.L. Porter, B.S.B. Christensen, and D. Wildenschild. Comparison of pressure-saturation characteristics derived from computed tomography and Lattice Boltzmann simulations. *Water Resour. Res.*, 43(W12S06), 2007.

[122] C. J. Seto, G. T. Tang, K. Jessen, A. R. Kovscek, and F. M. Orr. Adsorption Hys-

teresis and its Effect on CO2 Sequestration and Enhanced Coalbed Methane Recovery. *AGU Fall Meeting Abstracts*, pages D1542+, December 2006.

[123] Ji-Quan Shi, Saikat Mazumder, Karl-Heinz Wolf, and Sevket Durucan. Competitive methane desorption by supercritical CO2; injection in coal. *Transport in Porous Media*, 75:35–54, 2008. 10.1007/s11242-008-9209-9.

[124] J.Q. Shi and S. Durucan. A bidisperse pore diffusion model for methane displacement desorption in coal by CO2 injection. *Fuel*, 82:1219–1229, 2003.

[125] R. E. Showalter. *Monotone operators in Banach space and nonlinear partial differential equations*, volume 49 of *Mathematical Surveys and Monographs*. American Mathematical Society, Providence, RI, 1997.

[126] Hema J. Siriwardane, Raj K. Gondle, and Duane H. Smith. Shrinkage and swelling of coal induced by desorption and sorption of fluids: Theoretical model and interpretation of a field project. *International Journal of Coal Geology*, 77(1-2):188 – 202, 2009. CO2 Sequestration in Coals and Enhanced Coalbed Methane Recovery.

[127] E.D. Sloan and C. A. Koh. *Clathrate Hydrates of Natural Gases*. CRC Press, third edition, 2008.

[128] Sauro Succi. *The Lattice Boltzmann equation for fluid dynamics and beyond*. Numerical Mathematics and Scientific Computation. The Clarendon Press Oxford University Press, New York, 2001. Oxford Science Publications.

[129] C.E. Taylor, D. D. Link, and N. English. Methane hydrate research at NETL Research to make methane production from hydrates a reality. *JPSE*, 56:186–191, 2007.

[130] Colin J. Thompson. *Classical Equilibrium Statistical Mechanics*. Oxford Science Publishers, 1988.

[131] P. Tishchenko, C. Hensen, K. Wallmann, and C. S. Wong. Calculation of stability and solubility of methane hydrate in seawater. *Chemical Geology*, 219:37–52, 2005.

[132] Ioannis N. Tsimpanogiannis and Peter C. Lichtner. Parametric study of methane hydrate dissociation in oceanic sediments driven by thermal stimulation. *Journal of Petroleum Science and Engineering*, 56(1-3):165 – 175, 2007. Natural Gas Hydrate / Clathrate.

[133] Aslak Tveito and Ragnar Winther. On the rate of convergence to equilibrium for a system of conservation laws with a relaxation term. *SIAM J. Math. Anal.*, 28(1):136–161, 1997.

[134] Michael Ulbrich. *Semismooth Newton methods for variational inequalities and constrained optimization problems in function spaces*, volume 11 of *MOS-SIAM Series on Optimization*. Society for Industrial and Applied Mathematics (SIAM), Philadelphia, PA, 2011.

[135] Frank van Bergen, Pawel Krzystolik, Niels van Wageningen, Henk Pagnier, Bartlomiej Jura, Jacek Skiba, Pascal Winthaegen, and Zbigniew Kobiela. Production of gas from coal seams in the Upper Silesian Coal Basin in Poland in the post-injection period of an ECBM pilot site. *International Journal of Coal Geology*, 77(1-2):175 – 187, 2009. CO2 Sequestration in Coals and Enhanced Coalbed Methane Recovery.

[136] Augusto Visintin. *Differential models of hysteresis*, volume 111 of *Applied Mathematical Sciences*. Springer-Verlag, Berlin, 1994.

[137] G.X. Wang, X.R. Wei, K. Wang, P. Massarotto, and V. Rudolph. Sorption-induced swelling/shrinkage and permeability of coal under stressed adsorption/desorption conditions. *International Journal of Coal Geology*, 83(1):46 – 54, 2010.

[138] M.D. White, M. Oostrom, and R.J. Lenhard. Modeling fluid flow and transport in variably saturated porous media with the STOMP simulator. 1. Nonvolatile three-phase model description. *Advances in Water Resources*, 18(6), 1995.

[139] D. Wildenschild, K.A. Culligan, and B.S.B. Christensen. Application of x-ray microtomography to environmental fluid flow problems. In U. Bonse, editor,

*Developments in X-Ray Tomography IV*, volume 5535 of *Proc. of SPIE*, pages 432–441. SPIE, Bellingham, WA, 2004.

[140] Karl-Heinz A.A. Wolf, Frank van Bergen, Rudy Ephraim, and Henk Pagnier. Determination of the cleat angle distribution of the RECOPOL coal seams, using CT-scans and image analysis on drilling cuttings and coal blocks. *International Journal of Coal Geology*, 73(3-4):259 – 272, 2008.

[141] Dieter A. Wolf-Gladrow. *Lattice-Gas cellular automata and Lattice Boltzmann models*. Lecture Notes in Mathematics 1725. Springer, 2000.

[142] Hyung-June Woo and P. A. Monson. Phase behavior and dynamics of fluids in mesoporous glasses. *Phys. Rev. E*, 67(4):041207, Apr 2003.

[143] Hyung-June Woo, L. Sarkisov, and P. A. Monson. Mean-field theory of fluid adsorption in a porous glass. *Langmuir*, 17(24):7472–7475, 2001.

[144] W. Xu. Modeling dynamic marine gas hydrate systems. *American Mineralogist*, 89:1271–1279, 2004.

[145] W. Xu and C. Ruppel. Predicting the occurence, distribution, and evolution of methane hydrate in porous marine sediments. *Journal of Geophysical Research*, 104:5081–5095, 1999.

[146] J.M. Yeomans. *Statistical Mechanics of Phase Transitions*. Oxford, 1992.

[147] Son-Young Yi, Małgorzata Peszyńska, and Ralph Showalter. Numerical upscaled model of transport with non-separated scales. In *Proceedings of CMWR XVIII in Barcelona, June 21-24, 2010*. available online at http://congress.cimne.com/CMWR2010/Proceedings, 2010. paper 188.

[148] Hongguan Yu, Guangzhu Zhou, Weitang Fan, and Jianping Ye. Predicted CO2 enhanced coalbed methane recovery and CO2 sequestration in china. *International Journal of Coal Geology*, 71(2-3):345 – 357, 2007.

[149] Hongguan Yu, Lili Zhou, Weijia Guo, Jiulong Cheng, and Qianting Hu. Predictions of the adsorption equilibrium of methane/carbon dioxide binary gas on coals using Langmuir and Ideal Adsorbed Solution theory under feed gas conditions. *International Journal of Coal Geology*, 73(2):115 – 129, 2008.

[150] Katarzyna Zarebska and Grazyna Ceglarska-Stefanska. The change in effective stress associated with swelling during carbon dioxide sequestration on natural gas recovery. *International Journal of Coal Geology*, 74(3-4):167 – 174, 2008.